Subpicosecond Raman studies of electric-field-induced optical phonon instability in an $In_{0.53}Ga_{0.47}As$-based semiconductor nanostructure

2006 J. Phys.: Condens. Matter 18 7961

(http://iopscience.iop.org/0953-8984/18/34/009)

INSTITUTE OF PHYSICS PUBLISHING JOURNAL OF PHYSICS: CONDENSED MATTER

J. Phys.: Condens. Matter **18** (2006) 7961–7974 doi:10.1088/0953-8984/18/34/009

Subpicosecond Raman studies of electric-field-induced optical phonon instability in an $In_{0.53}Ga_{0.47}As$-based semiconductor nanostructure

K T Tsen[1], Juliann G Kiang[2,3], D K Ferry[4], V A Kochelap[5], S M Komirenko[6], K W Kim[6] and H Morkoc[7]

[1] Department of Physics and Astronomy, Arizona State University, Tempe, AZ 85287, USA
[2] Department of Cellular Injury, Walter Reed Army Institute of Research, Silver Spring, MD 20910-7500, USA
[3] Department of Medicine and of Pharmacology, Uniformed Services University of The Health Sciences, Bethesda, MD 20814-4799, USA
[4] Department of Electrical Engineering, Arizona State University, Tempe, AZ 85287, USA
[5] Department of Theoretical Physics, Institute of Semiconductor Physics, National Academic of Sciences of Ukraine, Kiev-28, 252650, Ukraine
[6] Department of Electrical and Computer Engineering, North Carolina State University, Raleigh, NC 27695-7911, USA
[7] Department of Physics and Electrical Engineering, Virginia Commonwealth University, Richmond, VA 23284, USA

Received 14 June 2006
Published 7 August 2006
Online at stacks.iop.org/JPhysCM/18/7961

Abstract

Transient carrier transport phenomena in an $In_{0.53}Ga_{0.47}As$-based p–i–n semiconductor nanostructure have been studied by using subpicosecond transient/time-resolved Raman spectroscopy. We observe an instability of the GaAs-like optical phonon population in this nanostructure semiconductor that occurs when electrons are accelerated to very high velocities by the application of intense electric fields. The results open up a new channel for creating coherent THz frequency that can be used in THz electronic devices. We suggest that the observed phenomena will have enormous impact on the carrier dynamics and carrier transport in nanoscale semiconductor electronic devices.

1. Introduction

Under the application of an intense electric field, electrons can be accelerated so that their drift velocity exceeds the sound velocity of the semiconductor, thus leading to the coherent emission of a large number of acoustic phonons. This so-called 'Cerenkov acousto-electric effect' was predicted [1, 2] and observed [3–6] in the 1960s in semiconductors with large piezoelectricity [3] such as CdS, and multivalley crystals with electron–phonon interaction via the deformation potential [5]. A similar effect, optical phonon instability, was also predicted [6–10] in the 1960s, and recently by Komirenko *et al* [11], and has been recently

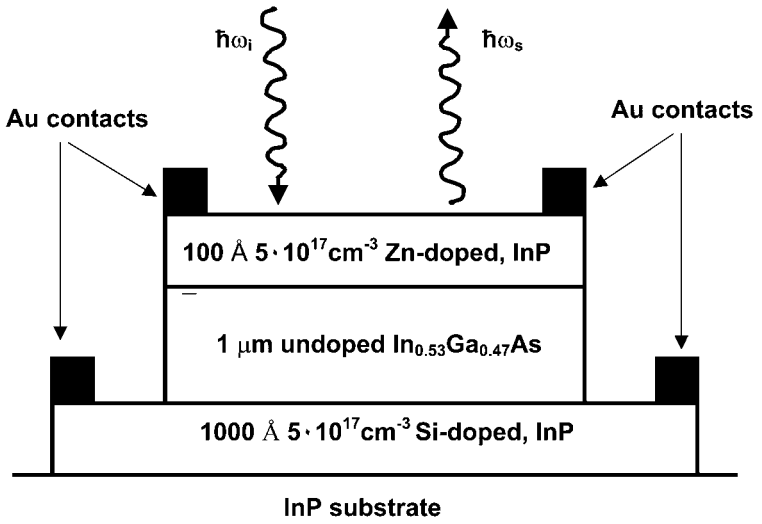

Figure 1. The $In_{0.53}Ga_{0.47}As$-based p–i–n semiconductor nanostructure used in our experiments. The reverse-biased condition is used so that electrons photoinjected inside the 1 μm-thick undoped $In_{0.53}Ga_{0.47}As$ layer traverse from the p-region toward the n-region.

demonstrated by Liang *et al* [12] in a GaAs-based semiconductor nanostructure. It is well known that optical phonons play a major role in the energy relaxation of fast (hot) electrons in semiconductors [13]. An optical phonon instability induced by hot electrons during their transport will have enormous impact on the carrier dynamics in semiconductor devices, particularly in nanostructure devices which inherently have large applied electric fields and electron drift velocities. In addition, the instability leads to amplification/generation of coherent optical phonons. It can be suggested that a number of applications will become possible on the basis of the electric methods of generation of coherent optical phonons.

In this work, we use subpicosecond Raman spectroscopy to study transient electron and phonon dynamics in an $In_{0.53}Ga_{0.47}As$-based p–i–n semiconductor nanostructure. An anomalous increase of the GaAs-like longitudinal optical (LO) phonon occupation number is observed when the applied electric field intensity is larger than 10 kV cm^{-1}. By correlating this experimental finding with electron distributions measured independently during the transient, we attribute this anomaly in the GaAs-like LO phonon population to the amplification/instability of LO phonons produced by electrons during their transient transport in the $In_{0.53}Ga_{0.47}As$-based p–i–n nanostructure.

2. Sample and experimental approach

The $In_{0.53}Ga_{0.47}As$-based nanostructure used in this work consisted of an InP–$In_{0.53}Ga_{0.47}As$–InP p–i–n structure grown by molecular beam epitaxy on a (001)-oriented InP substrate. As shown in figure 1, the p-type region is made up of a 100 Å-thick Zn-doped ($\cong 5 \times 10^{17}$ cm^{-3}) InP layer. The i-region is a 1 μm-thick intrinsic $In_{0.53}Ga_{0.47}As$ layer. This is the active region probed by our Raman scattering experiments. The n-type region consists of a 1000 Å-thick Si-doped ($\cong 5 \times 10^{17}$ cm^{-3}) InP layer. Gold contacts are established on both the p and n sides of the mesa-like p–i–n diode structure in order to apply an electric field. An opening of $\cong 0.25$ mm^2 in area is created in the gold layer on the p side of the diode so that light scattering experiments

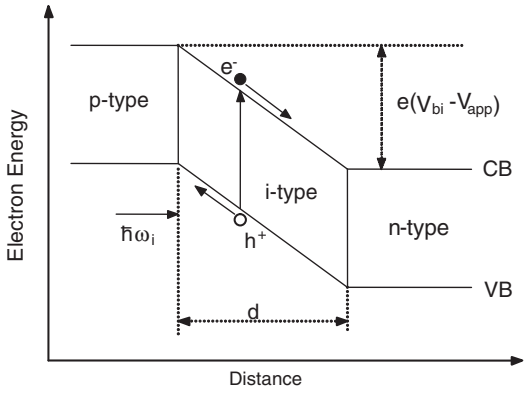

Figure 2. An electron energy diagram in real space for a typical p–i–n semiconductor nanostructure. CB, conduction band; VB, valence band. Electron–hole pairs are photo-injected into the intrinsic layer of the sample. Electrons and holes are accelerated by the existing electric field toward n-type and p-type layers, respectively.

can be carried out. The Zn-doped p-type layer and Si-doped n-type layer together serve as a capacitor and provide a uniform electric field across the active region of the sample.

The sample was excited and probed by a double-jet DCM dye laser that was synchronously pumped by the output of the second harmonic of a cw mode-locked YAlG laser [14]. The ultrafast laser, which has a pulse width of FWHM $\cong$ 800 fs, was operated at a repetition rate of 76 MHz, and with photon energy $\hbar\omega_{\rm L} \cong 1.95$ eV. In the case of transient experiments, i.e., the same laser pulse was used for both excitation and probing, the output from the dye laser was directed into the sample, whereas for time-resolved Raman experiments the dye laser was split into two equally intense, but perpendicularly polarized, beams. One of them was used to excite non-equilibrium excitations in the sample and the other, after being suitably delayed, was used to probe the evolution in time of non-equilibrium electron distributions and phonons. The backward-scattered Raman signal was collected and analysed by a standard Raman system which consisted of a double spectrometer, a photomultiplier tube (for measuring electron distributions) and a CCD detector (for measuring phonon populations). All the data reported here were taken at $T \cong 10$ K. The single-particle scattering (SPS) experiments, which were used to measure directly the electron distributions, were conducted in the $Z(X, Y)\bar{Z}$ scattering geometry, where $X = (100)$, $Y = (010)$ and $Z = (001)$. This scattering configuration ensures the detection of scattered light signal from only spin-density fluctuations (SDF) [15]. In order to easily observe non-equilibrium LO phonons, a $Z(X', X')\bar{Z}$ scattering geometry was used, where $X' = (110)$.

Figure 2 shows the electron energy diagram in real space for a typical p–i–n semiconductor nanostructure. Here, the effect of InP layers has been neglected for simplicity. The experimental idea here is that electron–hole pairs are first optically injected into the intrinsic region of the sample with a subpicosecond laser pulse; electrons are subsequently accelerated toward the n-region of the sample by the existing applied electric field. The non-equilibrium electron distributions, non-equilibrium phonon populations and electron drift velocities during the transient are then probed either by the same subpicosecond laser pulse (for transient experiments) or by a time-delayed laser pulse (for time-resolved experiments) through Raman spectroscopy. We note that since the wavevector transfer of the excitation photon is anti-parallel to the direction of applied electric field, our Raman scattering experiments probe electron distributions in the direction of electron transport. There are two important advantages of

probing non-equilibrium excitations with Raman spectroscopy. Firstly, since it detects Raman signal only when probing photons are present, its time-resolution is essentially limited by the pulse width of the ultrafast laser and not by the response of detection system. Secondly, Raman scattering cross section is inversely proportional to the square of the carrier's effective mass [16]; this property together with the fact that the effective mass of an electron is usually much smaller than that of a hole in semiconductors imply that Raman spectroscopy preferentially probes transport properties of electrons even though electrons and holes are simultaneously injected into the sample in our experiments.

2.1. Determination of the average effective electric field intensity under ultrashort pulse laser irradiation

In the study of high-field electron transport in semiconductors with optical techniques, a very challenging question always emerges—'how does one accurately measure the effective electric field intensity during the transient?'. All of the optical techniques involve the generation of electron–hole pairs. In our transient/time-resolved Raman studies of electron transport in semiconductor nanostructures, electron–hole pairs were photoexcited by an ultrashort laser pulse and subsequently underwent acceleration by the applied electric field. The effective electric field experienced by the traversing electrons inside the scattering volume might be expected to be different from the following simple equation [17]:

$$E = (V_{\mathrm{app}} - V_{\mathrm{bi}})/d; \tag{1}$$

where V_{app} and V_{bi} are the applied electric field and built-in electric field, respectively; d is the thickness of the intrinsic layer. This is because the spatial separation of electrons and holes during the transient generates an electric field which tends to oppose the applied electric field. In this section, in a similar way to reference [18], we describe briefly how the average effective electric fields under various applied electric field intensities and photoexcited electron–hole pair densities were obtained.

When an electric field is applied to a semiconductor, the electric field separates electron–hole pairs and modifies their wavefunctions from Bloch to Airy type. As a result, Raman scattering intensity of phonons in semiconductors oscillates as a function of the applied electric field [19]. This so-called Franz–Keldysh effect will be used in our Raman experiments to determine the average effective electric field under ultrashort pulsed laser irradiation.

In order to determine the effective electric field in the presence of photoexcited electron–hole pairs, we first perform Raman scattering measurements of LO phonons as a function of the applied electric field at a very low ($n \cong 10^{12}$ cm^{-3}) photoexcited electron–hole pair density with a cw laser. We note that for such a low photoexcited electron–hole pair density the effects of photoexcited carriers on the effective electric field are expected to be minimal, and the effective electric field during the transient should be very well described by equation (1). These experimental results were used as a calibration curve for the determination of effective electric field under ultrashort pulsed laser excitation. Secondly, subpicosecond Raman experiments were carried out in which LO phonon intensities were measured at the same average laser power and photon energy as in the cw case. Non-equilibrium phonon effects were properly taken into account by dividing the measured LO phonon Raman intensities by $(1 + \Delta n_{\mathrm{non-eq}})$, where $\Delta n_{\mathrm{non-eq}}$ was the non-equilibrium LO phonon occupation number generated under ultrashort pulsed laser excitations. By comparing these normalized LO phonon intensities with the calibration curve, the average effective electric field intensities under ultrashort pulsed laser excitations were deduced. We note that during the pulsed laser excitation the separation of photoexcited electrons and holes modifies the instantaneous electric field in the sample, which in turn alters the amount of separation of photoexcited electrons and holes.

2.2. Determination of the non-equilibrium phonon occupation number

The population of non-equilibrium LO phonons $n(\omega_{\mathrm{LO}})$ is obtained by comparing the measured Raman scattering intensity $I_{\mathrm{S}}(\omega_i)$ of the Stokes line (creation of a phonon) measured at photon energy $\hbar\omega_i$ with the intensity $I_{\mathrm{AS}}(\omega_i - \omega_{\mathrm{LO}})$ of the anti-Stokes line (absorption of a phonon) measured at photon energy $\hbar(\omega_i - \omega_{\mathrm{LO}})$. We obtain the phonon occupation number as [20]

$$n(\omega_{\mathrm{LO}}) = \left[\frac{I_{\mathrm{S}}(\omega_i)}{I_{\mathrm{AS}}(\omega_i - \omega_{\mathrm{LO}})} - 1\right]^{-1}. \tag{2}$$

However, we notice that when the experimental conditions are such that the photon energy $\hbar\omega_i$ is not in extreme resonance with any one of the energy gaps of a semiconductor then equation (2) can be shown to reduced to [20]

$$n(\omega_{\mathrm{LO}}) = \left[\frac{I_{\mathrm{S}}(\omega_i)}{I_{\mathrm{AS}}(\omega_i)} - 1\right]^{-1}; \tag{3}$$

which is a much simpler expression to obtain experimentally the non-equilibrium LO phonon populations. We have found that under our experimental conditions, the measured non-equilibrium LO phonon populations are the same using equation (2) as using (3).

2.3. Determination of non-equilibrium electron distributions

Raman scattering from electrons also exists—the so-called SPS, which is a manifestation of the Compton effect [21]. This scattering contribution provides a direct measurement of the non-equilibrium electron velocity distribution function in an applied electric field. From this distribution we determine the electron drift velocity in the field. We assume that electron distribution function is non-degenerate and neglect the momentum dependence of the matrix element and the effects of collision in the scattering cross section. We also assume an effective mass approximation. The SPS intensity $I_{\mathrm{e}}(\omega)$ associated with SDF in the relatively long probe pulse can be written as [22]

$$I_{\mathrm{e}}(\omega) = C\left(\frac{1}{m_{\mathrm{e}}^*}\right)^2 \int \mathrm{d}^3 p \cdot n(\vec{p}) \cdot \delta\left[\omega - \vec{V}\cdot\vec{q} - \frac{\hbar q^2}{2m_{\mathrm{e}}^*}\right]. \tag{4}$$

Here C is a constant, $\omega \equiv \omega_i - \omega_s$ is the energy transfer from light to electrons, and similarly $\vec{q} \equiv \vec{k}_i - \vec{k}_s$ is the wavevector transfer. The momentum distribution function for the electrons is $n(\vec{p})$, $\vec{V}$ is the electron velocity, and m_{e}^* is the electron effective mass.

This important result states that the number of electrons that have a velocity component V_q in the direction of wavevector transfer $\vec{q}$ is directly proportional to the measured Raman scattering cross section $I_{\mathrm{e}}(\omega)$ at a specific frequency shift ω and is inversely proportional to the square of the electron effective mass.

Since the effective mass of the electrons is not constant throughout the Γ-valley, non-parabolicity of the conduction band has been considered. In semiconductors such as GaAs, the higher the electron velocity in the Γ-valley, the higher its effective mass becomes. We appropriately [23] take this effect into account in our reported distribution functions.

3. Experimental results and analysis

The measured transient non-equilibrium GaAs-like LO phonon occupation number as a function of the applied electric field intensity for an $In_{0.53}Ga_{0.47}As$-based p–i–n nanostructure, taken at $T = 10$ K, is shown in figure 3. For a better illustration, results for a GaAs-based

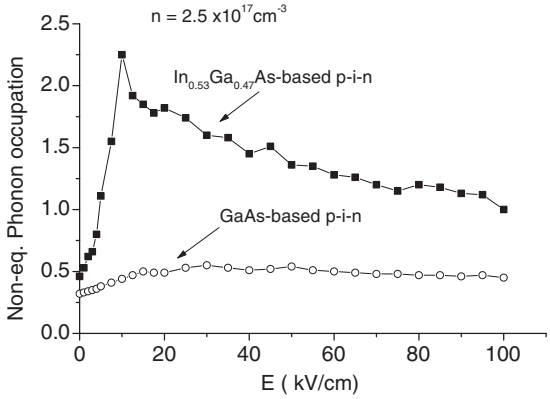

Figure 3. The measured non-equilibrium GaAs-like LO phonon occupation as a function of the applied electric field intensity for an $In_{0.53}Ga_{0.47}As$-based p–i–n nanostructure (solid squares). The injected electron–hole pair density is $n \cong 2.5 \times 10^{17}$ cm^{-3}. The abrupt increase of the non-equilibrium phonon population at $E = 10$ kV cm^{-1} is attributed to the detection of amplification of GaAs-like LO phonons. For comparison, non-equilibrium LO phonons for a GaAs-based p–i–n nanostructure, taken under the same experimental conditions, are also shown (open circles). The inset shows the details between 0 and 10 kV cm^{-1}.

p–i–n nanostructure taken under the same experimental conditions are also shown. The non-equilibrium LO phonon occupation number in a GaAs-based p–i–n nanostructure gradually increases as the electric field intensity increases to $\cong$10 kV cm^{-1}, and then almost flattens out as the electric field intensity increases beyond 10 kV cm^{-1}. This can be reasonably well explained by ensemble Monte Carlo (EMC) calculations that include conventional electron–phonon scattering [24]. In contrast, the non-equilibrium GaAs-like LO phonon occupation number for an $In_{0.53}Ga_{0.47}As$-based p–i–n nanostructure exhibits a very different behaviour. The non-equilibrium GaAs-like LO phonon population first increases smoothly as the applied electric field intensity increases up to $\approx$7.5 kV cm^{-1}. It increases very sharply to a maximum at $E \cong 10$ kV cm^{-1}, then decreases slowly to an almost constant value at an electric field intensity of $E = 60$ kV cm^{-1} and higher. Apparently, typical EMC calculations cannot account for this experimental finding.

Similar anomalous behaviour for InAs-like LO phonon populations as a function of the applied electric field intensity in the $In_{0.53}Ga_{0.47}As$-based p–i–n nanostructure have also been observed, which is not shown here.

We note that the effects of intervalley scattering will reduce the number of electron in the Γ-valley (and therefore, reduce the non-equilibrium LO phonon population) until about 1 ps [25–28]; however, because of their much heavier electron effective masses, the intra-X or intra-L valley electron relaxation emits much larger wavevector LO phonons than that probed in our experiments; therefore, the effects of intervalley scattering processes cannot account for our observed results. The penetration depth for the probe laser is shorter for $In_{0.53}Ga_{0.47}As$ than for GaAs. Under the application of an electric field, electrons acquire a significant drift velocity, and tend to escape from the probing volume of the laser. However, due to the consideration of the penetration depth, this effect will tend to reduce the measured GaAs-like LO phonon occupation in $In_{0.53}Ga_{0.47}As$ more than LO phonon population in GaAs; therefore, this cannot explain our experimental results.

Figure 4 shows GaAs-like LO phonon occupation number as a function of time delay for an $In_{0.53}Ga_{0.47}As$-based p–i–n nanostructure, taken at $E = 10$ kV cm^{-1}. For comparison,

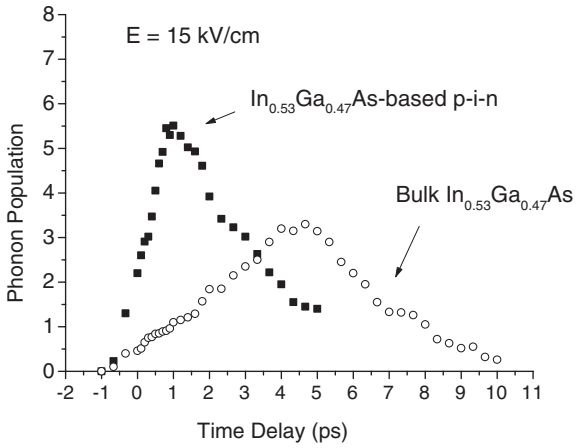

Figure 4. Integrated anti-Stokes GaAs-like LO phonons in an $In_{0.53}Ga_{0.47}As$-based p–i–n nanostructure as a function of time delay. For illustration, integrated anti-Stokes GaAs-like LO phonons in a bulk $In_{0.53}Ga_{0.47}As$ are also shown. See the text for discussions.

experimental results for a bulk $In_{0.53}Ga_{0.47}As$ sample are also shown. In contrast to the GaAs case [24], we have observed that (1) the non-equilibrium GaAs-like LO phonon population is significantly larger in an $In_{0.53}Ga_{0.47}As$-based p–i–n nanostructure than in a bulk $In_{0.53}Ga_{0.47}As$ sample and (2) the peak position of non-equilibrium GaAs-like LO phonon population occurs at a much earlier time for an $In_{0.53}Ga_{0.47}As$-based p–i–n nanostructure than for a bulk $In_{0.53}Ga_{0.47}As$ sample.

All of these new features and arguments suggest that under our transient carrier transport conditions there exists a new phonon generation mechanism. It is operating and being detected in our Raman experiments for an $In_{0.53}Ga_{0.47}As$-based p–i–n nanostructure but not in a GaAs-based p–i–n nanostructure. We attribute the anomalous increase of the phonon occupation observed in the $In_{0.53}Ga_{0.47}As$-based p–i–n nanostructure for electric field intensity $E \geqslant 10\ \mathrm{kV\,cm^{-1}}$ to the amplification/instability of GaAs-like LO phonons during the electron's transport from p- to n-regions.

In order to explain our experimental results, we evaluate the criterion of the optical phonon instability by using a macroscopic approximation, which is based on well known equations for the optical displacement $\vec{u}$, the polarization $\vec{P}$ and the field $\vec{E}$ [29]. We assume that $\vec{u}$, $\vec{P}$, $\vec{E}$ and ρ (the charge density) are proportional to $\exp(\mathrm{i}\vec{q}\cdot\vec{r} - \mathrm{i}\omega t)$. The total dielectric function that includes the lattice and electronic contributions are then calculated in the random phase approximation [30, 31]. The roots of the total dielectric function give rise to the angular frequency of the LO-plasmon coupled modes: $\omega_{\mathrm{LO}}(q)$. If it happens that this $\omega_{\mathrm{LO}}(q)$ has an imaginary part then one gets either damping (if the imaginary part is negative) or amplification (if the imaginary part is positive) of the mode.

It can be shown that the imaginary part of $\omega_{\mathrm{LO}}(q)$ for a polar semiconductor is given by [32]

$$\mathrm{Im}(\omega_{\mathrm{LO}}(q)) = -\gamma + \frac{2\pi e^2 n_{\mathrm{e}}\omega_{\mathrm{LO}}}{\hbar q^3}\left(\frac{1}{\varepsilon_\infty} - \frac{1}{\varepsilon_0}\right)\left[f\left(\frac{\omega_{\mathrm{LO}}}{q} + \frac{\hbar q}{2m_{\mathrm{e}}^*}\right) - f\left(\frac{\omega_{\mathrm{LO}}}{q} - \frac{\hbar q}{2m_{\mathrm{e}}^*}\right)\right]; \quad (5)$$

where $\omega_{\mathrm{LO}} \equiv \omega_{\mathrm{TO}}\sqrt{\frac{\varepsilon_0}{\varepsilon_\infty}}$; e is the charge of an electron; n_{e} is the electron density; $\hbar = h/2\pi$, h is Planck's constant, and f is the electron distribution function. ε_0, ε_∞ are the static and high

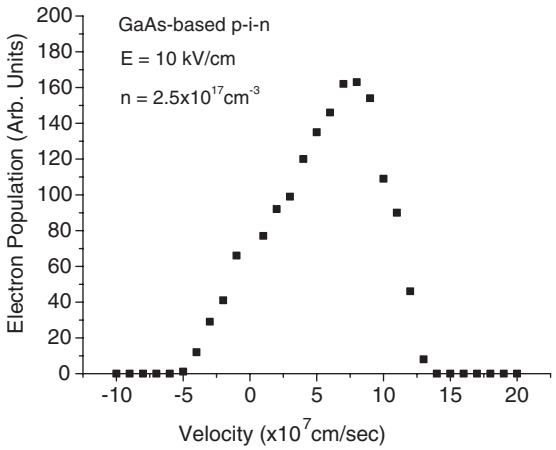

Figure 5. The measured non-equilibrium electron distribution for a GaAs-based p–i–n nanostructure, taken with electron–hole pair density $n \cong 2.5 \times 10^{17}$ cm^{-3}, and at $E = 10$ kV cm^{-1}.

frequency dielectric constants; $\omega_{\rm TO}$ is the angular frequency of the transverse optical phonons. γ is the phonon damping constant.

Therefore, the criterion of optical phonon instability becomes

$$\Gamma(q) \equiv \frac{2\pi e^2 n_{\rm e} \omega_{\rm LO}}{\hbar q^3}\left(\frac{1}{\varepsilon_\infty} - \frac{1}{\varepsilon_0}\right)\left[f\left(\frac{\omega_{\rm LO}}{q} + \frac{\hbar q}{2m_{\rm e}^*}\right) - f\left(\frac{\omega_{\rm LO}}{q} - \frac{\hbar q}{2m_{\rm e}^*}\right)\right] > \gamma. \tag{6}$$

For simplicity, if we ignore the phonon damping in equation (5)[8], then the theory predicts that the amplification/instability of optical phonons occurs when the drift velocity of the electrons exceeds the phase velocity of the optical phonons. In other words, because the dispersion of optical phonons in semiconductors is typically very small, for a given LO phonon with wavevector q to be amplified, the theory predicts that the minimum electron drift velocity is given by $(V_{\rm d})_{\rm min} = \frac{\omega_{\rm LO}}{q}$, where $\omega_{\rm LO}$ is the angular frequency of the LO phonon.

Based upon our discussions on optical phonon amplification/instability, we are now at a proper stage to explain our experimental findings in figure 3.

For the case of a GaAs-based p–i–n nanostructure, the index of refraction is about 3.4 [33], since the photon energy in the laser pulse is $\hbar\omega_i = 1.95$ eV, the LO phonon wavevector probed in our Raman experiments is $q \cong 6.70 \times 10^5$ cm^{-3}. The LO phonon energy is $\hbar\omega_{\rm LO} \cong 36.88$ meV. According to our theoretical analysis, the lower bound for the electron drift velocity in order that the amplified LO phonons can be detected in our Raman experiments would be $(V_{\rm d})_{\rm min} \cong 8.30 \times 10^7$ cm s^{-1}. On the other hand, independent measurements of electron distribution, and therefore electron drift velocity, in a GaAs-based p–i–n nanostructure as a function of the applied electric field have also been made. Results are shown in table 1. A typical non-equilibrium electron distribution obtained from our Raman experiments is shown in figure 5 for $E \cong 10$ kV cm^{-1}. We notice that within our experimental accuracy, the measured electron drift velocities are always smaller than the required minimum electron drift velocity required for LO phonon amplification. This explains why amplification of LO phonons in the GaAs-based p–i–n nanostructure was not detected in our Raman experiments.

[8] In fact, if we are to take the phonon damping into account, for a typical semiconductor, the minimum electron drift velocity $(V_{\rm d})_{\rm min}$ increases by about 5%.

Table 1. Measured electron drift velocity as a function of the applied electric field intensity in a GaAs-based p–i–n nanostructure at $T = 10$ K.

E (kV cm^{-1})	V_d ($\times 10^7$ cm s^{-1})
1	1.65 ± 0.1
2	2.30 ± 0.2
3	2.62 ± 0.2
4	2.95 ± 0.3
5	3.01 ± 0.3
7.5	3.80 ± 0.4
10	5.5 ± 0.5
12.5	5.6 ± 0.5
15	5.5 ± 0.5
20	5.7 ± 0.5
25	5.8 ± 0.5
30	6.0 ± 0.5
35	6.1 ± 0.5
40	6.2 ± 0.5
45	6.1 ± 0.5
50	6.0 ± 0.5
55	6.2 ± 0.5
60	6.3 ± 0.5
65	6.1 ± 0.5
70	6.0 ± 0.5
75	6.1 ± 0.5
80	6.0 ± 0.5
85	6.0 ± 0.5
90	6.1 ± 0.5
95	6.1 ± 0.5
100	6.0 ± 0.5

For the $In_{0.53}Ga_{0.47}As$-based p–i–n nanostructure, the index of refraction is about 4.0 [33]. The phonon wavevector probed in our Raman experiments is then given by $q \cong 7.89 \times 10^5$ cm^{-1}. The GaAs-like LO phonon energy is $\hbar\omega_{LO} \cong 34.13$ meV. This, based on our theoretical discussions, sets a lower bound for the electron drift velocity $(V_d)_{min} \cong 6.52 \times 10^7$ cm s^{-1} so that the amplified GaAs-like LO phonons can be observed in our Raman experiments. Table 2 shows the measured electron drift velocity as a function of the applied electric field intensity for the $In_{0.53}Ga_{0.47}As$-based p–i–n nanostructure. A typical non-equilibrium electron distribution obtained from our Raman experiments is shown in figure 6 for $E \cong 10$ kV cm^{-1}. It is obvious that for electric field intensities greater than or equal to 7.5 kV cm^{-1}, the electron drift velocities are larger than the required minimum electron drift velocity $(V_d)_{min}$ for GaAs-like LO phonon amplification/instability. As a result, instability/amplification of GaAs-like LO phonons is expected and should be detected in our Raman experiments. The detection of these amplified LO phonons is indeed observed in figure 3 in the form of a very rapid rise of GaAs-like LO phonon population for $E \geqslant 7.5$ kV cm^{-1}.

We note the following. (1) Because of the electron intervalley scattering processes, within the duration of our excitation pulse width ($\cong$800 fs), the number of electrons remaining in the Γ-valley becomes fewer as the applied electric field intensity increases. This means that under our experimental conditions the non-equilibrium GaAs-like LO phonon populations detected in the Raman measurements are expected to decrease when the electric field intensity increases, due to the electron intervalley scattering processes. (2) Once the electrons move out

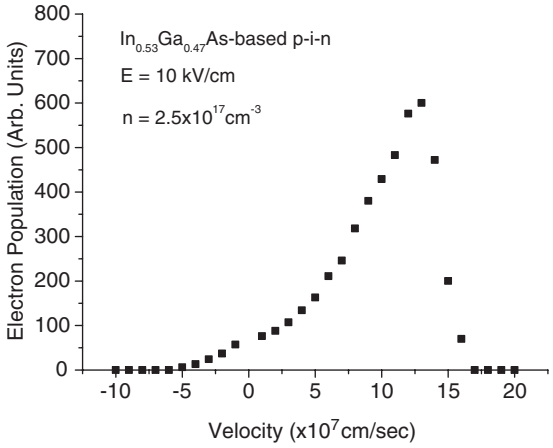

Figure 6. The measured non-equilibrium electron distribution for an $In_{0.53}Ga_{0.47}As$-based p–i–n nanostructure, taken with electron–hole pair density $n \cong 2.5 \times 10^{17}$ cm^{-3}, and at $E = 10$ kV cm^{-1}.

Table 2. Measured electron drift velocity as a function of the applied electric field intensity in an $In_{0.53}Ga_{0.47}As$-based p–i–n nanostructure at $T = 10$ K.

E (kV cm^{-1})	V_d ($\times 10^7$ cm s^{-1})
1	2.7 ± 0.2
2	4.0 ± 0.4
3	5.3 ± 0.5
4	5.9 ± 0.6
5	6.9 ± 0.6
7.5	8.5 ± 0.8
10	9.0 ± 0.9
12	9.5 ± 0.9
12.5	9.6 ± 0.9
15	9.9 ± 0.9
20	10.0 ± 1.0
25	10.2 ± 1.0
30	9.8 ± 0.9
35	10.4 ± 1.0
40	10.5 ± 1.0
45	10.2 ± 1.0
50	9.8 ± 0.9
55	10.0 ± 1.0
60	10.1 ± 1.0
65	9.6 ± 0.9
70	9.8 ± 0.9
75	9.9 ± 0.9
80	10.0 ± 1.0
85	10.1 ± 1.0
90	10.1 ± 1.0
95	10.0 ± 1.0
100	9.8 ± 0.9

of the scattering volume, the amplified GaAs-like LO phonons they generate will no longer be detected in our Raman experiments because of the fact that GaAs-like LO phonons have almost

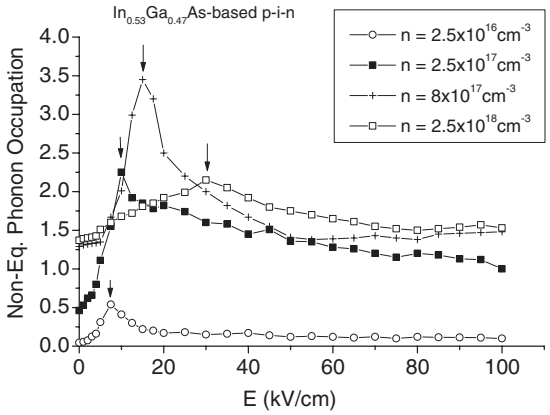

Figure 7. Non-equilibrium GaAs-like LO phonon occupation number as a function of the applied electric field for a variety of injected electron–hole pair densities, as indicated.

zero group velocity. We observe that electron drift velocity increases up to about 20 kV cm^{-1} and then almost flattens out (as shown in table 2). This implies that while the population of amplified GaAs-like LO phonons keeps increasing for fields up to 20 kV cm^{-1}, the effect of escaping from the scattering volume tends to offset the amount of the increase. The interplay between (1) and (2) just described explains why the non-equilibrium GaAs-like LO phonons first reaches a maximum at $E = 10$ kV cm^{-1}, and then gradually decreases as the electric field intensity increases beyond 10 kV cm^{-1}.

There are a couple of intriguing points in figures 5 and 6 that are worth mentioning: firstly, electron distributions cut off very rapidly around 1×10^8 cm s^{-1} and 1.4×10^8 cm s^{-1}, for GaAs-based and $In_{0.53}Ga_{0.47}As$-based p–i–n nanostructures, respectively. This is an indication of the effect of non-parabolicity of the band structure and the onset of electron intervalley scattering processes in these semiconductors [21]. Secondly, electron drift velocity is substantially higher for the $In_{0.53}Ga_{0.47}As$-based p–i–n nanostructure than for the GaAs-based p–i–n nanostructure. This is primarily due to the much larger $\Gamma \rightarrow L$ intervalley separation in the former ($\widetilde{=}$0.6 eV) than in the latter ($\widetilde{=}$0.35 eV) [34].

In order to further test our interpretation, we have carried out similar Raman experiments for the $In_{0.53}Ga_{0.47}As$-based p–i–n nanostructure for a variety of injected electron–hole pair densities. The results are shown in figure 7. We note that the electric field intensity around which amplification of GaAs-like LO phonons occurs (as indicated by the arrows) increases when the injected electron–hole pair density increases. These observations are consistent with our understanding that electron drift velocity decreases as the injected electron–hole pair density increases for a given applied electric field intensity [21].

4. Discussions

To obtain a simple physical insight into the phenomenon of optical phonon amplification by the accelerated electrons, we first note that equation (5) can be rewritten as

$$\mathrm{Im}[\omega_{\mathrm{LO}}(q)] = -\gamma + D\int \mathrm{d}^3k\,[f(\vec{k}) - f(\vec{k}+\vec{q})]\delta[\varepsilon(\vec{k}+\vec{q}) - \varepsilon(\vec{k}) - \hbar\omega]; \tag{7}$$

where D is a constant; $\varepsilon(\vec{k})$ is the electron energy at $\vec{k}$ and $f(\vec{k})$ is the electron distribution function. The δ-function insures energy conservation, $\hbar\omega = \varepsilon(\vec{k}+\vec{q}) - \varepsilon(\vec{k})$, in the transition of an electron from $\varepsilon(\vec{k})$ to $\varepsilon(\vec{k}+\vec{q})$.

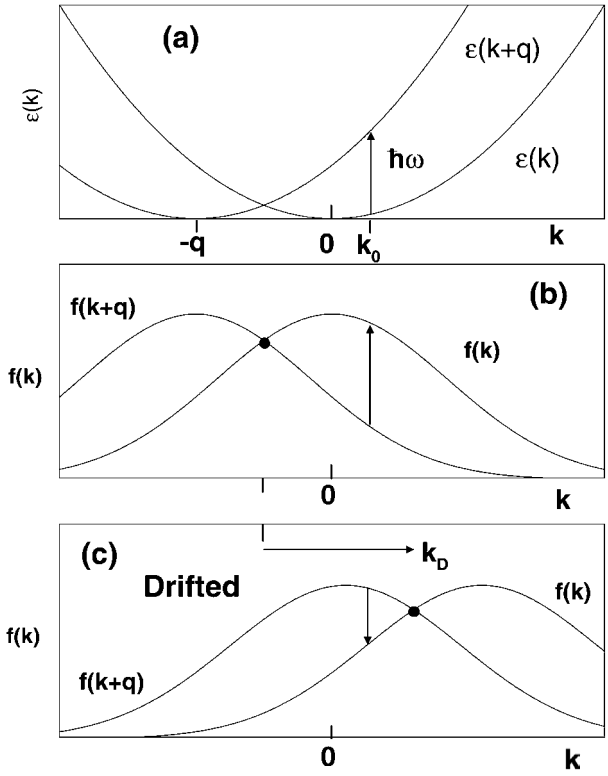

Figure 8. A schematic diagram for a fixed (q, ω) pair that illustrates the absorption or the emission of energy by the electron gas. Absorption is produced by the undrifted distribution and emission (into the phonon subsystem) is generated by the drifted electron distribution. (a) Conservation of energy occurs between the two free electron parabolas, $\varepsilon(k+q)$ and $\varepsilon(k)$. Energy conservation occurs at the k-value k_0; (b) two distribution functions, $f(k)$ and $f(k+q)$, similar to MB distributions that are centred at $k = 0$ (no drift). The quantity $f(k_0) - f(k_0+q)$ is positive (upward pointed vertical arrow) indicating net energy being absorbed by the electron system; (c) the drifted distributions $f(k)$ and $f(k+q)$ that are drifted by an amount k_D. At k_0, there exists now a population inversion with $f(k_0) - f(k_0+q)$ being negative (downward pointing vertical arrow) indicating net energy emitted by the electron system.

The energy exchange between the phonon and electron systems changes its direction from phonon damping to phonon amplification when the sign of $\mathrm{Im}[\omega_{\mathrm{LO}}(q)]$ changes from positive to negative. Phonon amplification can be seen to occur by considering a Maxwell–Boltzmann (MB) distribution function for the electrons; similar results are obtained for a Fermi–Dirac distribution. The two terms in equation (7) (one involving $f(\vec{k})$ and one involving $f(\vec{k}+\vec{q})$), and the conditions under which they produce phonon damping or amplification, are illustrated in figure 8. This discussion assumes fixed values of ω and q corresponding to a specific optical phonon. For simplicity, we also assume that there is no damping for optical phonons, i.e. $\gamma \equiv 0$. Figure 8(a) shows how the condition of energy conservation (δ-function in equation (7)) between free-electron-like states $\varepsilon(k+q)$ and $\varepsilon(k)$ is satisfied. A transition from $\varepsilon(k+q)$ to $\varepsilon(k)$ (or vice versa) occurs at a unique value of k_0 ($=m_e^*\omega/\hbar q - q/2$) and is indicated by the vertical arrow. When the electron distribution is at equilibrium, the number of transitions upward is greater than the number downward ($f(k) - f(k+q) > 0$), as can be seen in figure 8(b) for an equilibrium (undrifted Gaussian) MB distribution. Equation (7) then

shows $\mathrm{Im}[\omega_{\mathrm{LO}}(q)] > 0$ for an equilibrium MB distribution, so that energy is absorbed by the electron gas from the phonons and phonons are damped.

If we create a non-equilibrium population inversion where $f(k) - f(k+q) < 0$, energy will be pumped out of the electron system ($\mathrm{Im}[\omega_{\mathrm{LO}}(q)] < 0$) and into the phonon system. This will occur for a population inversion at that specific (q, ω) pair. Figure 8(c) shows MB distributions that include a drift, where the drift in k-space is equal to k_{D}. When we compare figure 8(b) with figure 8(c) we note that the position where the two ($f(k)$ and $f(k+q)$) distributions are equal (indicated by the 'dot') is moved to the right in figure 8(c) due to the drift. In fact, the drift shown is large enough that the 'dot' moves to the right of k_0. This is the key criterion. When this circumstance occurs, the electron population becomes inverted ($f(k) - f(k+q) < 0$), and we obtain amplification of these (q, ω) LO phonons. The condition for amplification is quite simply that the 'dot' moves from $-q/2$ for the equilibrium distribution to anywhere to the right of k_0. The minimum k_{D} for this to occur is $k_{\mathrm{D}} > k_0 + q/2$. It is a simple exercise to evaluate this minimum k_{D}, and the condition for amplification of a phonon at (q, ω) is $V_D > \omega/q$, and $V_D = \hbar k_{\mathrm{D}}/m_{\mathrm{e}}^*$ is the electron drift velocity. In words, for this simple demonstration, the condition for optical phonon amplification is that the drift velocity of the carriers must be higher than the phase velocity of the phonons. This condition is in fact reminiscent of the condition for Cerenkov radiation, where the velocity of a particle in the medium is greater than the phase velocity of light in that medium. It is also similar to the condition for a sonic boom of a jet airplane.

In semiconductor nanostructure devices, electron transport is primarily governed by electron velocity overshoot effects [21]; as a result, electron drift velocity can usually be as high as 10^8 cm s^{-1}. This extremely high electron drift velocity means that optical phonon modes will be amplified for a wide range of the phonon wavevectors. The phonons with the smallest wavevectors from this wavevector interval can under some appropriate circumstances be probed by Raman spectroscopy, as demonstrated in this work. Since the strength of Fröhlich interaction is inversely proportional to the square of phonon wavevector [35], for nanostructures of size $\geqslant$500 Å in which quantum confinement effects are minimal, our experimental results suggest that instability of LO phonons will have an enormous impact on the carrier dynamics and transport in semiconductor nanostructure devices.

5. Conclusion

Electric-field-induced non-equilibrium electron and phonon dynamics have been studied in an $In_{0.53}Ga_{0.47}As$-based p–i–n nanostructure by using subpicosecond Raman spectroscopy. Instability/amplification of GaAs-like LO phonons have been observed. The experimental results are consistent with a macroscopic theory which takes into account the many body effects through the random phase approximation. We demonstrate that instability can be achieved for LO phonon modes whose phase velocity is smaller than the electron drift velocity. Our experimental findings will have an enormous impact on the carrier dynamics in semiconductor nanostructure devices.

Acknowledgment

This work is supported by the National Science Foundation under grant No DMR-0305147.

References

[1] Weinreich G 1956 *Phys. Rev.* **104** 321
[2] Tolpygo K B and Uritskii Z I 1956 *J. Exp. Theor. Phys.* **30** 929

[3] Hutson A R, McFee J H and White D L 1961 *Phys. Rev. Lett.* **7** 237
[4] Toxen A M and Tansal S 1963 *Phys. Rev. Lett.* **10** 481
[5] Pomerants M 1964 *Phys. Rev. Lett.* **13** 308
[6] For a review, see Spector H N 1966 *Solid State Phys.* **19** 291
[7] Gurevich V L 1962 *Sov. Phys.—Solid State* **4** 1015 (Engl. Transl.)
[8] Yokota I 1964 *Phys. Lett.* **10** 27
[9] Chaban I A and Chaban A A 1964 *Sov. Phys.—Solid State* **6** 1913 (Engl. Transl.)
[10] Gunn J B 1964 *Phys. Rev.* **138** A1721
[11] Komirenko S M *et al* 2002 *Proc. 2nd IEEE Conf. on Nanotechnology (Washington, DC, Aug. 2002)* (Piscataway, NJ: IEEE) p 1
[12] Liang W, Tsen K T, Sankey O F, Komirenko S M, Kim K W, Kochelap V A, Wu M C, Ho C L, Ho W J and Morkoc H 2003 *Appl. Phys. Lett.* **82** 1968
[13] Shah J 1992 *Hot Carriers in Semiconductors* ed J Shah (Boston: Academic) p 279
[14] Tsen K T, Wald K R, Ruf T, Yu P Y and Morkoc H 1991 *Phys. Rev. Lett.* **67** 2557–60
[15] Klein M V 1983 *Light Scattering in Solids I* vol 8 *Topics in Applied Physics* ed M Cardona (New York: Springer) p 151
[16] Abstreiter G, Cardona M and Pinczuk A 1986 *Light Scattering in Solids IV* ed M Cardona and G Güntherodt (New York: Springer) p 5
[17] Shields A J, Trallero-Giner C, Cardona M, Grahn H T, Ploog K, Haisler V A, Tenne D A, Moshegov N T and Poropov A I 1992 *Phys. Rev.* B **46** 6990
[18] Tsen K T, Joshi R P, Salvador A, Botcharev A and Morkoc H 1997 *J. Appl. Phys.* **81** 406
[19] Kuball M, Esser N, Ruf T, Ulrich C, Cardona M, Ebert K, Garcia-Cristobal A and Cantarero A 1995 *Phys. Rev.* B **51** 7253
[20] See for example Yu P Y and Cardona M 1996 *Fundamentals of Semiconductors* (New York: Springer)
[21] Tsen K T 2001 *Ultrafast Phenomena in Semiconductors* ed K T Tsen (New York: Springer) p 191
[22] Chia C, Sankey O F and Tsen K T 1993 *Mod. Phys. Lett.* B **7** 331
[23] Ruf T and Cardona M 1990 *Phys. Rev.* B **41** 10747
[24] Grann E D, Tsen K T, Ferry D K, Salvador A, Botcharev A and Morkoc H 1997 *Phys. Rev.* B **56** 9539–44
[25] Kim D S and Yu P Y 1991 *Phys. Rev.* B **43** 4158
[26] Bigot J-Y, Portella M T, Schoenlein R W, Cunningham J E and Shank C V 1990 *Phys. Rev. Lett.* **65** 3429
[27] Shah J, Deveaud B, Damen T C, Tsang W T, Gossard A C and Lugli P 1987 *Phys. Rev. Lett.* **59** 2222
[28] Elsaesser T, Shah J, Rota L and Lugli P 1991 *Phys. Rev. Lett.* **66** 1757
[29] Born M and Huang K 1954 *Dynamic Theory of Crystal Lattices* (New York: Oxford University Press)
[30] Platzman P M and Wolff P A 1973 *Waves and Interactions in Solid State Plasmas* (*Solid State Physics* Supplement # 13) (New York: Academic)
[31] Kittel C 1963 *Quantum Theory of Solids* (New York: Wiley)
[32] Komirenko S M, Kim K W, Kochelap V A, Fedorov I and Stroscio M A 2001 *Phys. Rev.* B **63** 165308
[33] Palik E D 1985 *Handbook of Optical Constants of Solids* ed E D Palik (New York: Academic) p 429
[34] Liang W, Tsen K T, Ferry D K, Wu M-C, Ho C-L and Ho W-J 2003 *Appl. Phys. Lett.* **83** 1438–40
[35] Conwell E M 1967 *High Field Transport in Semiconductors* (New York: Academic)